Saudi Pharmaceutical Journal 31 (2023) 101792

HOSTED BY

Contents lists available at ScienceDirect

Saudi Pharmaceutical Journal

journal homepage: www.sciencedirect.com

Original article

Gu-Ben-Hua-Shi (AESS) formula ameliorates atopic dermatitis via regulating NLRP3 signaling pathways

Xiong Li [a,1], Luyao Feng [b,1], Tingjing Zhong [a], Xiumei Mo [c], Dong Wang [b], Jiangyong Gu [d], Dacan Chen [c,*], Xing Zeng [a], Fenggen Yan [c,*]

[a] The Second Clinical College of Guangzhou University of Chinese Medicine, Guangzhou, Guangdong Province 510120, China
[b] School of Traditional Chinese Medicine, Shenyang Pharmaceutical University, Shenyang, Liaoning Province 117000, China
[c] State Key Laboratory of Dampness Syndrome of Chinese Medicine, The Second Affiliated Hospital of Guangzhou University of Chinese Medicine (Guangdong Provincial Hospital of Chinese Medicine), Guangzhou, Guangdong Province 510120, China
[d] The Research Centre of Integrative Medicine, School of Basic Medical Science, Guangzhou University of Chinese Medicine, Guangzhou 510006, China

ARTICLE INFO

Article history:
Received 15 June 2023
Revised 11 September 2023
Accepted 13 September 2023
Available online 21 September 2023

Keywords:
Atopic dermatitis
Traditional Chinese medicine
UHPLC-MS/MS
NLRP3 signaling pathway

ABSTRACT

Background: Gu-ben-hua-shi (AESS) formula is a clinical experienced prescription from Guangdong Hospital of Traditional Chinese Medicine (TCM), which is used to treat atopic dermatitis (AD). Our previous work has shown that AESS has therapeutic effect on AD by regulating yes-associated protein (YAP). AESS formula has multi-component and multi-target characteristic, and need to be analyzed by systematic chemical profiling and network pharmacology technology, as well as verification of key signaling pathways. Therefore, this study aimed at investigating the efficacy and effect of AESS formula in the treatment of AD and its effect on NLRP3 signaling pathway.

Methods: The components of AESS formula were analyzed and identified by ultra high performance liquid chromatography/tandem mass spectrometry (UHPLC- MS/MS), and the potential mechanism of AESS formula in the treatment of AD was predicted by network pharmacology approach, with detected main components, and the potential components targeted NOD-like receptor thermal protein domain associated protein (NLRP3) signaling pathway [Direct binding with NLRP3, apoptosis-associated speck-like protein (ASC) and Caspase-1] were assessed using molecular docking. AD-like symptoms were constructed by DNCB induced BALB/c mice. The effect of AESS formula on dorsal skin structure in AD-like mice was observed using H&E staining. Furthermore, the western blotting experiment explored the expression of the NLRP3 pathway protein.

Results: By UHPLC-MS/MS analysis, 91 compounds were detected in AESS formula, and 76 of them were identified, while by network pharmacological analysis, 1500 component targets were obtained, and 257 of them were obtained by intersection with eczema targets. Then one of the key pathways, nucleotide-binding oligomerization domain (NOD)-like signaling pathway was obtained by KEGG enrichment analysis. Molecular docking results showed 24 main components could effectively combine with ASC and Caspase-1 (≤ -7 kcal/mol). The animal experiment results further showed that AESS formula alleviates symptoms in AD-like mice. ELISA kit results showed that the expression of IL-1β and IL-18 in serum was inhibited after AESS treatment. Additionally, western blotting analysis showed that the expressions of ASC, Caspase-1 and NLRP3 protein expression in the skin tissue of mice were down-regulated after

Abbreviations: AESS, Gu-Ben-Hua-Shi; NLRP3, NOD-like receptor thermal protein domain associated protein; TCM, Traditional Chinese Medicine; AD, atopic dermatitis; YAP, yes-associated protein; UHPLC-MS/MS, ultra high performance liquid chromatography/tandem mass spectrometry; ASC, apoptosis-associated speck-like protein; NOD, Nucleotide-binding oligomerization domain; NLRs, nucleotide-binding and oligomerization domain-like receptors; FLG, filaggrin; PPI, protein–protein interaction; AO, acetone-olive oil; H&E, Hematoxylin-eosin; ELISA, Enzyme linked immunosorbent assay; OD, optical density; TIC, total ion chromatography; BP, biological processes; CC, cellular components; MF, molecular functions; DEX, dexamethasone; PRRs, Pattern recognition receptors; NK, natural killer.

* Corresponding authors.
E-mail addresses: cdc@gzucm.edu.cn (D. Chen), fenggen_yan@gzucm.edu.cn (F. Yan).

[1] These authors have contributed equally to this work.

Peer review under responsibility of King Saud University.

Production and hosting by Elsevier

https://doi.org/10.1016/j.jsps.2023.101792

AESS treatment. The experimental results show that AESS formula inhibited the expression of NLRP3 signaling pathway for the treatment of AD.
Conclusions: AESS formula can improve AD symptoms in mice by inhibiting the activation of NLRP3 inflammasome and the expression of the related downstream inflammatory cytokines.

1. Introduction

Atopic dermatitis (AD), also known as eczema, is a common clinical inflammatory skin disease caused by a variety of factors, clinically manifested by severe pruritus, erythema, papules, lichen skin lesions and so on (Jiang et al., 2018). Due to the rapid growth of population and the aggravation of environmental pollution, the incidence of AD has increased. Each year, up to 17.1% of adults and 22.6% of children were diagnosed with AD, including 9.6% new cases of AD in children (Bylund et al., 2020). So the prevention and treatment of AD is one of the hot topics of medical focus.

It is reported that nucleotide-binding and oligomerization domain-like receptors (NLRs) play essential roles in various autoimmune diseases. NLRs are divided into five subfamilies, namely NLRA, NLRB, NLRC, NLRP and NLRX. NLRP and NLRC are the two major subfamilies that are found to be relevant to allergic diseases, including AD and allergic asthma, while NLRP3 is the most important inflammasome in the NLRP subfamily. NLRP3 usually forms inflammatory bodies with the adaptor protein apoptosis-associated speck-like protein (ASC) and an inactive zymogen pro-Caspase-1 (Tsang et al., 2021). The assembled inflammasome induces the processing of the effector protein Caspase-1 and subsequently promotes the cleavage of inactive precursors pro-IL-1β and pro-IL-18 into pro-inflammatory cytokines IL-1β and IL-18 (Swanson et al., 2019). IL-1β is significantly elevated in skin blisters of patients with AD that have filaggrin gene (FLG) mutation and and in the skin of $Flg^{ft/ft}$ mice (Schwartz et al., 2018), and IL-18 level was found to be elevated in the serum of AD patients and NC/Nga mice during the development of AD (Tanaka et al., 2001). It has been demonstrated that activating the NLRP3 inflammatories in keratinocytes and promoting the release of downstream pro-inflammatory cytokines may be a risk factor for AD (Zheng et al., 2021). Therefore, inhibition of NLRP3 inflammasome may be an effective treatment strategy for AD.

At present, the clinical drugs treatment of AD is mainly divided into chemical synthetic drugs and traditional folk medicine. Chemical medicine usually uses topical drugs, such as glucocorticoids for external use, which has anti-inflammatory, anti-allergic, and immunosuppressive effects, may cause serious side effects, such as sleep disorders, skin pain, drug dependence, etc. Therefore, an increasing number of patients are asking for plant-based therapeutic products as complementary dermatologic therapy (Reuter et al., 2010). Traditional Chinese Medicine (TCM) is an alternative therapy that can be used in the treatment for dermatologic disorders, including AD and psoriasis (Koo et al., 2003). The Gu-ben-hua-shi (AESS) formula is the clinical experience prescription of professor Chen Dacan from Guangdong Hospital of TCM, and has been used to treat AD. According to TCM theory, Lonicerae Japonicae Flos was acted as the 'Monarch drug', Sophorae Flos and Curcumae Rhizoma were acted as 'minister drugs', Atractylodis Macrocephalae Rhizoma, Atractylodis Rhizoma, Rehmanniae Radix and Coicis Semen were acted as 'assistant drug', Saposhnikoviae Radix was acted as the 'guide drug', but the specific mechanism of action is still unclear. Our team's previous work has shown that AESS formula can regulate Th1/Th2/Th17/Treg immune balance and through the interaction of YAP and NF-κB signaling pathway (Jia et al., 2022). The purpose of this study was to further investigate the therapeutic material basis and intervention mechanism of AESS formula in the treatment of AD, and to verify the mechanism through network pharmacology and pharmacological experiments *in vivo*.

2. Material and methods

2.1. Preparation of AESS decoction

The prescribed herbs were purchased from different Chinese herbal medicine markets (Table 1). The plant names in AESS are checked with https://www.theplantlist.org. The standard information is shown in Supplemental Table S1. According to traditional decoction preparation process, the herbs were added to 10 times volume of water and boiled for 1 h, then concentrated at 60 °C under reduced pressure, and freeze-dried to obtain lyophilized powder. 5.0 mg of the freeze-dried powder was accurately weighed, 80% MeOH was added, and dissolved by ultrasound for 30 min. Then the final solvent was diluted with equal volume ultra-pure water, and the final solvent was 40% MeOH. After centrifugation at 13000 rpm for 10 min, the supernatant solution was filtered through a 0.22 μm filter membrane, and taken into sample bottle (5 mg/ml). Then placed at 4 °C for use. The standard was accurately weighed and prepared into 5 μg/ml standard solution with 40%MeOH, which was placed at 4 °C for reserve.

2.2. UHPLC-MS conditions

An Dionex Ultimate HPLC 3000 coupled with QE-Orbitrap mass spectrometer was used in the analytical method development. (Thermo-Fisher, USA). Chromatographic methanol and acetonitrile were produced by Merck (Darmstadt, Germany), and formic acid was produced by Kermeo Chemical Reagent Co., Ltd. (Tianjin, China). The Hypersil GOLD (100 × 2.1 mm, 1.9 μm) column (Thermo Fisher Scientific,USA) was used. Mobile phase: 0.1% formic acid water (A)–acetonitrile (B). Gradient elution: 0–2 min, 5% B; 2–42 min, 5–95%B; 42–47 min, 95%B; 47–47.1 min, 95–5%B; 47.1–50 min, 5%B. Flow rate: 0.3 ml/min. The sample injection volume was 5 μL. The temperature of the column was 40 °C. The mass spectrometer was equipped with an electrospray ionization (ESI) interface operated in both positive and negative ion mode. Scanning range: 100.0–1500.0 *m/z*. Ion source temperature: 320 °C; The resolution was set at 70,000; The capillary voltage was 3.5 kV in the (+) ESI mode and −3.2 kV in the (−) ESI mode.

2.3. Network pharmacological analysis

2.3.1. Collection and screening of active components and targets of AESS

According to the results of composition analysis of serum after administration (Jia et al., 2022) and the qualitative results of UHPLC-MS/MS analysis, 37 compounds were selected for network pharmacological analysis. Component targets were collected using TCMSP (https://old.tcmspe.com/tcmspsearch.php/), SymMap

Table 1
The summarised information of composed herbs for AESS.

Botanical name	English name	Batch number	Place of origin	Dose (/g)*
Saposhnikovia divaricata (Turcz. ex Ledeb.) Schischk.	Saposhnikoviae Radix	2007001	Heilongjiang province	10
Coix lacryma-jobi L. var. mayuen (Roman.) Stapf	Coicis Semen	181105921	Guizhou province	20
Curcuma kwangsiensis S.G.Lee & C.F.Liang	Curcumae Rhizoma	191203761	Guangxi province	10
Atractylodes macrocephala Koidz.	Atractylodis Macrocephalae Rhizoma	1810002	Zhejiang province	15
Lonicera japonica Thunb.	Lonicerae Japonicae Flos	1911002	Shandong province	10
Rehmannia glutinosa Libosch.	Rehmanniae Radix	191000039	Henan province	10
Sophora japonica L	Sophorae Flos	200901	Jiangsu province	10
Atractylodes lancea (Thunb.) D C.	Atractylodis Rhizoma	191004471	Inner Mongolia Autonomous Region	10

* Drug usage (g) for each herb in AESS formula.

(https://www.symmap.org/search/), BATMAN-TCM (https://bionet.ncpsb.org.cn/batman-tcm/), Swiss Target Pred-iction (https://www.swissadme.ch/) and TCMIP (https://www.tcmip.cn/TCMIP/index.php/Home/Analysis/personal_center.html). Then input them into Uniport database (https://www.uniprot.org/) to convert the target protein information into standard gene marker na-mes.

2.3.2. Collection and screening of AD targets

The disease target of AD was obtained from GeneCards database (https://www.genecards.org/), DisGeNET database (https://www.disgenet.org/), TTD database (https://data-base.idrb.cqu.edu.cn/), TCMIP database and CTD database (https://ctdbase.org) with the keyword "eczema" as the search term. Then input them into Uniport database (https://www.uniprot.org/) to convert the target protein information into standard gene marker names.

2.3.3. Construction of protein–protein interaction network (PPI)

Input the disease target and component target into the draw Venn Diagram website (https://bioinformatics.psb.ugent.be/webtools/Venn/), establish the Venn Diagram and obtain the intersection targets. The intersection targets of AESS were analyzed in the STRING database (https://string-db.org), selected the Multiple proteins option, and Homo sapiens in Organization, adjusted the confidence to 0.7 and hid the disconnected nodes in the network. Then obtained the PPI and downloaded the target interaction network diagram and data. Input it into Cytoscape 3.8.2 software and used Network Analyzer function to analyze network topology.

2.3.4. GO enrichment analysis and KEGG enrichment analysis

GO and KEGG enrichment analysis of key target proteins were performed using DAVID database (https://david.ncifcrf.gov/), according to $P < 0.05$ was screened, and the results were analyzed visually.

2.3.5. Network of herbs -active components -targets -main pathways of AESS

The herbs, components, key targets, and key pathways were input into Cytoscape 3.8.2 software to build the "herbs-components-targets-pathways" Network, and Network Analyzer was used to analyze the network topology.

2.3.6. Molecular docking

The 3D structure of target protein, human NLRP3 (Uni Prot ID: Q96P20), human ASC (Uni Prot ID: Q9ULZ3) and Caspase-1 (Uni Prot ID: P29466), were downloaded from the Uni Prot database (https://www.uniprot.org), then the software Pymol was used to remove ligands and solvent molecules, and AutoDock4.2 software was used for hydrogenation and electron addition. The binding energy was defined as ≤ -7 kcal/mol as the screening criterion.

2.4. Experimental verification of influence of NLRP3 pathway in AD

2.4.1. Animals

48 SPF healthy male BALB/c mice (20 ± 2 g, age: 6–8 weeks) were raised in Guangdong Provincial Hospital of Chinese Medicine, and the temperature was maintained at 22 ± 3 °C, and the relative humidity was 55 ± 5%. Adaptive feeding was carried out seven days before the experiment, and water and food were freely eaten. Random number method was used to group 6 groups, each group of 8 mice. It included control group, model group (AD), AESS low dose group (AESS0.5), AESS medium dose group (AESS1), AESS high dose group (AESS2) and dexamethasone group (DEX). The experimental animal ethics committee of the GuangdongProvincial Hospital of Chinese Medicine approved all experiments (No. 2021086).

2.4.2. Establishment of the AD-like mouse model

Before modeling, all mice's back skin tissues were depilated. After hair removal, the back skin was sensitized with 200 μL 1% DNCB (Sigma-Aldrich, USA) dissolved in acetone-olive oil (AO, 3:1). Control group were treated with vehicle. Then, the back skin was then sensitized with 200 μL 0.5% DNCB three times a week. The dosage of AESS formula is 14.41/kg/d, which is set as the middle dosage group, the low dosage group is 1/2 of the middle dosage group, and the high dosage group is 2 times of the middle dosage group. The positive group was given dexamethasone solution, 3.0 mg/kg orally daily. Start with the first stimulation once a day for 3 weeks. The changes of body weight and dermatitis score of mice were monitored during modeling.

2.4.3. Experimental model evaluation

The changes of body weight and dermatitis score of mice were monitored during modeling. On the 1st, 7th, 14th and 21st days of the experiment, the back skin lesions of mice in each group were observed, including erythema/haemorrhage, oedema, excoriation/erosion, and scaling/dryness and photographed and recorded. The severity of back lesions was graded on the following scale: 0 = none, 1 = mild, 2 = moderate, 3 = s evere.

2.4.4. Hematoxylin-eosin (H&E) staining

The back skin of mice in each group was fixed in 4% paraformaldehyde (the ratio of skin to fixed liquid was 1:8–1:10), and sent to the company for routine dehydration, fixation, paraffin embedding, sectioning, H&E staining, sealing, observation under the microscope, photo preservation.

2.4.5. Enzyme linked immunosorbent assay (ELISA)

According to the ELISA kit instructions, after the reaction was terminated, the optical density (OD value) of each hole was measured with an enzyme marker at 450 nm, and the data was input into Origin 2018 to establish a standard curve, calculate the sample concentration and statistical results.

2.4.6. Western blotting analysis

A certain amount of skin tissue was weighed and cleaved on ice with RIPA lysate containing PMSF for 30 min and centrifuged at 13000 rpm at 4 °C for 15 min. The protein concentration in skin tissue was determined by BCA protein concentration determination kit. After denatalization, the protein was separated by SDS-PAGE and transferred to PVDF membrane. 5% skim milk (dissolved in BSA reagent) was sealed for 2 h, and the corresponding diluted antibody was added for overnight incubation at 4 °C. The antibody was: ASC/TMS1(1:2000, CST, USA), Caspase-1(1:1000, CST, USA), NLRP3(1:500, CST, USA), and corresponding secondary antibodies were added and incubated at room temperature for 1 h, and imaging was performed by Image Lab 5.2.1 software. GAPDH (1:1000, CST, USA) as the internal standard.

2.4.7. Statistical analysis

Statistical software IBM SPSS Statistics 25 was used for data analysis, and Graph Pad Prism 8.0 (San Diego, CA, USA) was used for data mapping. The quantitative data are expressed as the mean ± SD. One-way analysis of variance and LSD test were used. $P < 0.05$ is considered statistically significant.

3. Results

3.1. Chemical composition analysis of AESS

A total of 91 components were detected and 76 components were identified in AESS, including 9 flavonoids, 11 organic acids, 6 phenylethanoid glycosides, 24 terpenoids, 12 diarylheptanoids and 14 other components. 47 of them were compared with standards. The other compounds were identified according to literature and database comparison, and the results are shown in Table 2**.** The total ion chromatography (TIC) in positive and negative ion modes is shown in Fig. 1. The main components include chlorogenic acid, cryptochlo- rogenic acid, isochlorogenic acid A, isochlorogenic acid C, rutin, narcissoside, cmicifugoside, kaempferol-3-rutinoside and 4′-O-beta-D-Glucosyl-5-O-methylvisamminol, etc.

3.2. Network pharmacological analysis

3.2.1. Active components and eczema targets of AESS

Combined with the qualitative analysis results of AESS formula and absorbed components analysis, 37 compounds were selected as potential active components to obtain 1500 component targets, 1396 CE targets, and 257 intersection targets, as shown in Fig. 2A of Venn Diagram. The components related to the intersection target were screened out by using the intersection target, and one component (Isoacteoside) without common target was eliminated.

3.2.2. The PPI network of AESS

The interaction between targets of AESS in the treatment of AD was analyzed based on String database. Intersection targets were input and data was imported into Cytoscape 3.8.1 for visualization analysis (Fig. 2B). The results showed that there were 227 nodes and 1554 edges. Sorted according to the Degree value, the larger the degree value, the larger the node, the darker the color (green to red), and the wider the line width. It can be seen from the figure that the degree value of AKT1, TP53, TNF, JUN, IL-6, RELA, MAPK3, SRC, EGFR, VEGFA, IL-1β and other targets were larger. They may be the key targets of AESS in the treatment of AD.

3.2.3. GO analysis and KEGG pathway enrichment analysis

The intersection targets were imported into DAVID online database for GO and KEGG enrichment analysis. 681 GO enrichment analysis results were obtained (P Value < 0.01), including 495 biological processes (BP), 79 cellular components (CC) and 107 molecular functions (MF). The top 10 items of each item are selected for visual analysis, and the results are shown in Fig. 3A. The results suggest that AESS prescription may interact with these outcomes, influencing these biological processes and thereby exerting corresponding molecular functions to achieve the therapeutic effect of eczema. KEGG enrichment analysis showed that 144 pathways (P Value < 0.01), and the first 25 pathways were selected for visual analysis according to the size of P value and the degree of correlation with disease, and the results were shown in Fig. 3B. It mainly involves TNF signaling pathway, IL-17 signaling pathway, HIF-1 signaling pathway, Toll-like receptor signaling pathway, NF-κB signaling pathway, NOD-like receptor signaling pathway, etc.

3.2.4. Herb-component-target-pathways interactive network

Herbs, components, key targets, and 25 pathways were imported into Cytoscape software for visualization analysis, and the results were shown in Fig. 4. There are 325 nodes and 1108 edges in the figure. The orange hexagon represents the analyzed ingredients in Table 2, the pink square represents the pathway, the yellow triangle represents the herbal medicine, and the green circle represents the target. The larger the node, the greater the corresponding Degree value. The thicker the connection between nodes, the closer the connection between them.

3.2.5. Molecular docking

The molecular docking results showed that 24 main components could effectively combine with NLRP3, ASC and Caspase-1. Among them, chromones flavonoids, Cimicifugoside (37) had the strongest affinity for NLRP3 and ASC protein (−10.90 and −8.69 kcal/mol, respectively), while its aglycone, Cimifugin (47) had the strongest affinity for Caspase-1 protein (−7.62 kcal/mol) (Fig. 5). Other flavonoids, such as Quercetin(67), Luteoloside(42), Isoquercitrin (41), Narcissoside (51), Kaempferol-3-Rutinoside (48), Lonicerin (44), 4′-O-beta-D-Glucosyl-5-O-methylvisamminol (56), Sec-O-glucosyl- hamaudol (68), iridoid glycosides, including Sweroside (30), Epivogeloside (35), Secologanic acid (22), Morroniside (17), 8-Epi- Loganic acid (11), Loganin (29) and Vegeloside (28), cafeoyl quinic acid derivatives, including Isochlorogenic acid A (52), Isochlorogenic acid C (57), Chlorogenic acid (16), Neochlorogenic acid(7) and Cryptochlorogenic acid (18), and sesquiterpene, Zederone (82) and Germacrone (90), all had good affinity (≤−7 kcal/mol), indicating these components may exert anti-inflammatory activity through targeting NLRP3 signaling pathway.

3.3. Animal experiment

3.3.1. Body weight change

The body weight change of mice were recorded weekly during modeling, as shown in Fig. 6A. The results showed that the body weight of the administration group increased after the beginning of membrane building, thus the drug had no obvious toxicity to mice.

3.3.2. Dermatitis score

In order to evaluate the therapeutic effect of AESS formula on eczema-like mice, we took photos and compared the skin lesions of mice in each group, and statistically analyzed the measured results (Fig. 6B, C). No significant changes were observed in the control group before and after membrane construction. In the model group, the back skin of mice gradually showed obvious eczema symptoms such as erythema, oedema, bleeding, dryness,

Table 2
Analysis results of chemical compounds in AESS.

No.	t_R (min)	Experimental mass	Detection mode	Error (ppm)	Main fragment ions	Molecular Formula	Identification	Category	Resources	Ref.
1#	1.24	191.01872	–	−5.27	173.00784,129.01794,111.00735,	$C_6H_8O_7$	Citric Acid	Organic acids	AMR	*
2	1.27	268.10455	+	1.94	136.06207,268.10208,119.03558	$C_{10}H_{13}N_5O_4$	Adenosine	Nucleoside	CS	*
3#	2.06	166.08658	+	−0.45	120.08120,103.05477	$C_9H_{11}NO_2$	L-Phenylalanine	Amino acids	AR	*
4	2.58	153.01790	–	−2.20	153.01801,109.02808	$C_7H_6O_4$	Protocatechuic acid	Organic acids	SF	*
5	2.62	393.13977	–	−5.61	393.13803,127.03858,234.52377	$C_{15}H_{24}O_9$	Leonuride	Terpenoids	RR	TCMSP
6	3.09	127.03885	+	−2.30	127.03935,109.02878	$C_6H_6O_3$	5-hydroxymethyl furfural	Furaldehyde	Ad	*
7#	3.14	353.08737	–	−1.23	191.05499,135.04381,161.02293,179.03884	$C_{16}H_{18}O_9$	Neochlorogenic acid	Organic acids	LJF	*
8	3.79	205.09714	+	−1.80	146.06038,118.06561,188.07050	$C_{11}H_{12}O_2N_2$	D-tryptophan	Amino acids	AR	*
9	4.12	137.02307	–	−2.41	137.02307,109.02784,119.01232	$C_7H_6O_3$	Protamine sulfate	Organic acids	LJF	Li et al. (2019)
10#	4.24	345.11859	–	−1.49	299.11224,119.04854,59.01255	$C_{14}H_{20}O_7$	Salidroside	Glycosides	LJF	*
11#	4.46	375.12927	–	−1.07	151.07533,69.03310,95.04869	$C_{16}H_{24}O_{10}$	8-Epi-Loganic acid	Terpenoids	RR	*
12	5.24	449.12933	–	−1.63	416.35358,150.26289,139.00277	$C_{18}H_{26}O_{13}$	Unknown	Unknown	LJF	
13#	5.32	375.12903	–	−1.71	375.12943,113.02301,95.04888	$C_{16}H_{24}O_{10}$	Loganic acid	Terpenoids	LJF	*
14	5.40	471.22098	+	1.87	453.20734,291.15701,203.05284	$C_{21}H_{36}O_{10}$	Atractyloside A	Glycosides	AR	Zhang et al. (2019b)
15	5.42	493.22864	–	−0.83	447.22415,285.16980,89.02297	C_{22} H_{38} O_{12}	(1R,4S,6R)-1,3,3-trimethyl-2-oxabicyclo[2.2.2]oct-6-yl-6-O-β-D-glucopyranosyl-β-D-glucopyranoside	Glycosides	AMR,AR	Yang et al. (2012)
16#	5.74	353.08701	–	−2.17	191.05504,85.02805,173.04411	$C_{16}H_{18}O_9$	Chlorogenic acid	Organic acids	LJF	*
17#	5.85	451.14462	–	−2.42	155.03357,243.09,101.02298	$C_{17}H_{26}O_{11}$	Morroniside	Terpenoids	RR	*
18#	6.09	353.08734	–	−1.32	191.05499,135.04384,173.04424,161.02293	C_{16} H_{18} O_9	Cryptochlorogenic acid	Organic acids	LJF	. *
19	6.11	375.12900	–	−0.67	375.12866,201.01515,121.06453,89.02291,59.01252	C_{16} H_{24} O_{10}	Unknown	Unknown	LJF	
20	6.12	197.08124	+	2.05	179.07062,127.03935,111.08093	C_{10} H_{12} O_4	Xanthoxylin	Phenols	LJF	Li et al. (2022a)
21	6.45	389.10852	–	−1.07	69.03304,95.04860,121.06445,389.10806,314.66028	C_{16} H_{22} O_{11}	Unknown	Unknown	LJF	
22#	6.71	373.11322	–	−2.14	59.01252,97.02798,193.04890	$C_{16}H_{22}O_{10}$	Secologanic acid	Terpenoids	LJF	*
23	7.06	507.17133	–	−1.18	507.17093,191.05510,95.04880	$C_{21}H_{32}O_{14}$	Unknown	Unknown	LJF	
24	7.18	697.21808	–	−2.10	697.21765,341.10855,179.05511	C_{28} $H_{43}O_{20}$	Unknown	Unknown	LJF	
25	7.22	353.08731	–	−1.40	191.05515,179.0339885.02806	C_{16} $H_{17}O_9$	Unknown	Organic acids	LJF	
26	7.39	337.09192	–	−0.97	191.05511,119.04886,163.03883,93.03311	C_{16} $H_{18}O_8$	5-*p*-coumaroylquinic acid	Organic acids	LJF	Li et al. (2022a)
27	7.40	447.15012	–	−1.25	401.14505,269.10620,101.02297	C_{19} H_{28} O_{12}	Unknown	Unknown	LJF	
28#	7.60	433.13443	–	−1.66	387.20322,225.07568,101.02296	$C_{17}H_{24}O_{10}$	Vegeloside	Terpenoids	LJF	*
29#	7.73	435.15002	–	−1.37	101.02304,227.09172,127.03857	$C_{17}H_{26}O_{10}$	Loganin	Terpenoids	LJF	*
30#	7.76	403.12381	–	−1.92	125.02296,81.03316,376.25455	$C_{16}H_{22}O_9$	Sweroside	Terpenoids	LJF	*
31	7.78	345.15503	–	−1.77	165.09082,59.01247,71.01229, 89.02283,179.05455,345.15460	$C_{16}H_{26}O_8$	RehMapicroside	Terpenoids	RR	Zhao et al. (2007)
32	8.23	367.103	–	−0.46	191.05505,173.04446,134.03596,93.03311	$C_{17}H_{20}O_9$	3-O-feruloylquinic acid	Organic acids	LJF	Li et al. (2022a)
33	8.48	785.25000	–	−1.23	161.02321,785.24902,133.02814	C_{35} H_{46} O_{20}	Echinacoside	Phenylethanoid glycosides	RR	*
34	8.57	435.14999	–	−1.86	101.02304,157.04935,69.03306	$C_{17}H_{26}O_{10}$	Unknown	Unknown	LJF	
35#	8.62	433.13437	–	−1.80	123.04407,155.03326,424.50870	$C_{17}H_{24}O_{10}$	Epivogeloside	Terpenoids	LJF	*
36#	8.70	403.12378	–	−2.00	121.02808,59.01253,95.04877	$C_{17}H_{24}O_{11}$	Secoxyloganin	Terpenoids	LJF	*
37#	8.98	469.17148	+	−1.30	469.16974,307.11700	C_{22} $H_{28}O_{11}$	Cimicifugoside	Chromones	SR	*
38	9.35	799.26544	–	−1.62	179.05460,623.21759,161.02341, 461.16934,315.10806,135.04376	C_{36} $H_{48}O_{20}$	Jionoside A1	Phenylethanoid glycosides	RR	*
39	9.47	538.22980	+	0.77	141.05482,228.10222,376.17453	$C_{26}H_{35}O_{11}$ N	Unknown	Unknown	CS	
40#	9.51	609.14484	–	−2.08	609.14496,301.03574,271.02460,151.00282	$C_{27}H_{30}O_{16}$	Rutin	Flavonoids	SF	*
41#	9.78	463.08780	–	−0.86	463.08777,271.02448,300.02707,255.02933,151.00250	$C_{21}H_{20}O_{12}$	Isoquercitrin	Flavonoids	SF	*
42#	9.99	447.09265	–	−1.42	285.03998,447.09256	$C_{21}H_{20}O_{11}$	Luteoloside	Flavonoids	LJF	*
43	10.00	438.23969	+	−0.30	147.04393,204.10175	$C_{25}H_{31}O_4N_3$	Unknown	Unknown	CS	
44#	10.15	593.15051	–	−1.15	593.15045,285.03995	$C_{27}H_{30}O_{15}$	Lonicerin	Flavonoids	LJF	*
45	10.16	435.22433	–	−0.95	435.22433,383.97205,71.01240	$C_{20}H_{36}O_{10}$	Unknown	Unknown	RR	
46#	10.22	623.19714	–	−1.61	161.02318,135.04381,623. 19666,461.16678,315.10797	$C_{29}H_{36}O_{15}$	Verbascoside	Phenylethanoid glycosides	RR	*
47#	10.33	307.11810	+	−0.80	259.05975,235.05974,307.11694	C_{16} H_{18} O_6	Cimifugin	Chromones	SR	*
48#	10.43	593.15063	–	−0.83	255.02942,284.03229,227.03423	$C_{27}H_{30}$ O_{15}	Kaempferol-3-Rutinoside	Flavonoids	SF	*

(*continued on next page*)

Table 2 (*continued*)

No.	t_R (min)	Experimental mass	Detection mode	Error (ppm)	Main fragment ions	Molecular Formula	Identification	Category	Resources	Ref.
49	10.53	743.23975	–	−0.19	743.23926,203.03419,101.02301	$C_{46}H_{36}O_8N_2$	Unknown	Unknown	LJF	
50#	10.58	813.28070	–	−1.93	175.03888,160.03537,134.03596,637.23291,497.17712	$C_{37}H_{50}O_{20}$	Jionoside B1	Phenylethanoid glycosides	RR	*
51#	10.66	623.16003	–	−2.77	315.05060,300.02695,272.03085,151.00206	$C_{28}H_{32}O_{16}$	Narcissoside	Flavonoids	RR	*
52#	10.66	515.11847	–	−2.12	191.05507,135.04379	$C_{25}H_{24}O_{12}$	Isochlorogenic acid A	Organic acids	LJF	*
53	10.77	507.20776	–	−1.09	461.20074,255.02832,268.19434	$C_{21}H_{34}O_{11}$	Unknown		LJF	
54#	10.77	623.19702	–	−1.15	161.02318,133.02811,623.19775	$C_{29}H_{36}O_{15}$	Isoacteoside	Phenylethanoid glycosides	SF	*
55	11.08	403.16064	+	−0.6	109.02896,165.05496	$C_{18}H_{26}O_{10}$	Icariside F2	Flavonoids	LJF	
56#	11.15	453.17645	+	2.25	291.12317,273.11249,231.06560,245.11766,203.07080	$C_{22}H_{28}O_{10}$	4′-O-beta-D-Glucosyl-5-O-methylvisamminol	Chromones	SR	*
57#	11.40	515.11871	–	−1.28	191.05508,135.04381,173.04436	$C_{25}H_{24}O_{12}$	Isochlorogenic acid C	Organic acids	LJF	*
58	11.54	803.26044	–	−3.32	525.16046,285.03989	$C_{34}H_{46}O_{19}$	Centauroside or isomer	Terpenoids	LJF	TCMSP
59	11.64	331.15469	–	−1.23	331.15518,96.95868,122.03590	$C_{19}H_{24}O_5$	4-(3,5-dihydroxy-7-(4-hydroxyphenyl)heptyl) benzene-1,2-diol	Diarylheptanoids	CR	Chang et al. (2020)
60	11.81	361.16550	–	−0.45	151.03873,346.14185,361.16531	$C_{20}H_{26}O_6$	Unknown		RR	
61	11.84	331.15479	–	−0.93	331.15491,122.03595	$C_{19}H_{24}O_5$	4-(3,5-dihydroxy-7-(4-hydroxyphenyl)heptyl) benzene-1,2-diol isomer	Diarylheptanoids	CR	
62	12.01	803.26080	–	−1.28	101.02301,525.16174,595.20209	$C_{34}H_{46}O_{19}$	Centauroside or isomer	Terpenoids	LJF	TCMSP
63	12.13	523.18170	–	−0.76	134.03600,160.01537,193.04961,175.03883	$C_{25}H_{32}O_{12}$	6-O-E-Feruloylajugol	Terpenoids	RR	Lu et al. (2023)
64	12.37	577.15619	–	−0.47	145.02818,119.04876,163.03880	$C_{27}H_{30}O_{14}$	Unknown	Unknown	SF	
65	12.99	651.22845	–	−1.53	160.01537,175.03885,651.22821	$C_{31}H_{40}O_{15}$	Martynoside/ Isomartyside	Phenylethanoid glycosides	RR	Wei et al. (2022)
66	13.01	317.06278	+	1.56	317.06278,281.15466,187.11211, 147.08072,133.06508,107.04976	$C_{19}H_{24}O_4$	1,7-bis(4-hydroxyphenyl) heptane-3,5-diol	Diarylheptanoids	CR	Chang et al. (2020)
67#	13.26	301.03485	–	−1.75	151.00240,301.03491	$C_{15}H_{10}O_7$	Quercetin	Flavonoids	SF	*
68#	14.01	439.16101	+	2.59	259.09689,277.10745,231.10150,205.04994	$C_{21}H_{26}O_{10}$	Sec-O-glucosylhamaudol	Chromones	SR	*
69	14.02	389.15994	–	−1.64	329.13895,389.15985	$C_{21}H_{26}O_7$	1,7-bis(3,4-dihydroxyphenyl)-5-hydroxyheptan-3-yl acetate	Diarylheptanoids	CR	Li et al. (2021)
70	15.26	313.14404	–	−1.57	313.14386,121.02812,165.05424	$C_{19}H_{22}O_4$	(E)-4-(3-hydroxy-7-(4-hydroxyphenyl)hept-6-enyl)benzene-1,2-diol	Diarylheptanoids	CR	Chang et al. (2020)
71#	15.53	375.18085	+	−0.92	297.14828,357.16925	$C_{21}H_{26}O_6$	1-(3,4-dihydroxyphenyl)-5-hydroxy-7-(4-hydroxyphenyl)heptan-3-yl acetate	Diarylheptanoids	CR	*
72	15.60	315.05063	–	−1.35	300.02707,315.09036,151.00240,272.03253	$C_{16}H_{12}O_7$	Isorhamnetin	Flavonoids	CR	*
73	16.70	431.17020	–	−2.18	311.12845,431.17053,189.09099	$C_{23}H_{28}O_8$	1,7-bis(3,4-dihydroxyphenyl)heptane-3,5-diyl diacetate	Diarylheptanoids	CR	Chang et al. (2020)
74#	16.96	297.14914	–	−1.61	191.10663,132.05673	$C_{19}H_{22}O_3$	(3S)-/(3R)-1,7-Bis(4-hydroxyphenyl)-(6E)-6-hepten-3-ol	Diarylheptanoids	CR	*
75	17.11	357.17010	–	−1.81	315.15979,149.05957,191.10678	$C_{21}H_{26}O_5$	(3S)-and (3R)-3-acetoxy-1-(3,4-dihydroxyphenyl)-7-(4-hydroxy-phenyl) heptanes	Diarylheptanoids	CR	Chang et al. (2020)
76	17.94	295.10040	–	5.01	187.00595,295.10049	$C_{19}H_{20}O_3$	(E)-1,7-bis(4-hydroxyphenyl)hept-6-en-3-one	Diarylheptanoids	CR	Chang et al. (2020)
77#	18.02	293.11807	–	−0.95	119.04884,187.07542	$C_{19}H_{18}O_3$	1,7-bis(4-hydroxyphenyl) hepta-4E-6E-dien-3-one	Diarylheptanoids	CR	*
78#	18.38	415.17551	–	−1.65	415.17514,295.13333	$C_{23}H_{28}O_7$	1-(3,4-dihydroxyphenyl)-7-(4-hydroxyphenyl)heptane-3,5-diyl diacetate	Diarylheptanoids	CR	*

Table 2 (*continued*)

No.	t_R (min)	Experimental mass	Detection mode	Error (ppm)	Main fragment ions	Molecular Formula	Identification	Category	Resources	Ref.
79	20.15	235.16975	+	−0.41	161.09636,177.12775	$C_{15}H_{22}O_2$	Curcumenol	Terpenoids	CR	Li et al. (2022b)
80	20.68	183.08089	+	2.45	153.07014,155.41937,115.05470,129.07040	$C_{13}H_{11}O$	Atractylodin	Polyacetylene	AR	Zhang et al. (2019c)
81	20.69	249.14905	+	−0.65	231.13834,203.14326,189.12729,175.07576, 163.07558,119.08596,105.07042	$C_{15}H_{20}O_3$	Atractylenolide III	Terpenoids	AMR	Dong et al. (2020)
82#	20.87	247.13348	+	−0.40	139.03929,121.02888,229.12254	$C_{15}H_{18}O_3$	Zederone	Terpenoids	CR	*
83	22.30	779.45746	–	−1.61	779.45685,439.35782	$C_{42}H_{68}O_{13}$	Azukisaponin I	Terpenoids	SF	TCMSP
84	23.61	233.15315	+	−0.20	233.15343,187.14783	$C_{15}H_{20}O_2$	Atractylenolide II	Terpenoids	AR,AMR	*
85	23.70	217.15919	+	−2.76	217.15926,161.09633,199,14853	$C_{15}H_{20}O$	Atractylone	Terpenoids	AMR	Zhou et al. (2020)
86	23.83	231.13850	+	−2.39	83.08630,231.13853,213.12781	$C_{15}H_{18}O_2$	Curzerenone/ Furanodienone	Terpenoids	CR	Li et al. (2022b)
87	24.27	379.15237	+	1.63	153.07016,128.06241,115.05471,197.09637,	$C_{23}H_{23}O_5$	Unknown	Unknown	AMR	
88	25.20	199.07587	+	−3.18	146.96158,125.00292,181.06540	$C_{13}H_{10}O_2$	Atractylodinol	Terpenoids	AR	Dong et al. (2020)
89	18.39	231.13744	+	0.19	231.13745,213.12738,203.14333,185.13300,143.08588,	$C_{15}H_{18}O_2$	Atractylenolide I	Terpenoids	AMR,AR	*
90#	27.30	219.17482	+	−0.05	88.03899,146.08095,201.16383	$C_{15}H_{22}O$	Germacrone	Terpenoids	CR	Li et al. (2022b)
91	32.34	203.17993	+	0.53	203.17993,175.14859,161.13289,147.11716,133.10150	$C_{15}H_{22}$	Dehydrocitrene	Terpenoids	AMR	Zhong et al. (2015)

Notes: Atractylodis Macrocephalae Rhizoma: AMR. Atractylodis Rhizoma: AR. Curcumae Rhizoma: CR. Lonicerae Japonicae Flos: LJF. Sophorae Flos: SF. Rehmanniae Radix: RR. Coicis Semen: CS. Saposhnikoviae Radix: SR. Ad: Artificial derivative; The column of Ref. "*" represent identified by standards, others referred to references or databases. "#" represent component selected for network pharmacology.

erosion and scab due to DNCB application, and the dermatitis score gradually increased with the test time. In the AESS or DEX group, the symptoms of mice were significantly improved, and on day 21, the dermatitis score of mice was significantly lower than that of the model group, indicating that AESS formula and DEX had a good therapeutic effect on DNCB induced mice.

3.3.3. Histopathology

To investigate whether AESS formula could ameliorate the DNCB-induced animal model of AD, a histological examination (H&E) showed that epidermal thickness was reduced upon treatment with AESS formula. In addition, AESS formula treatment also significantly reduced the infiltration of eosinophils, lymphocytes, mononuclear cells and inflammatory cells into dorsal skin lesions (Fig. 7A). Moreover, in histopathological assessment of skin sections of mice intact structure and clear subcutaneous were observed in control group. Compared with the model group, DNCB application produced marked epidermal thickening. As we expected, AESS formula group (especially the medium dose AESS1 group) and the DEX group were significantly decreased inflammatory cell infiltration. The results indicated that AESS formula suppressed the symptoms of DNCB-induced AD model.

3.3.4. AESS inhibited the expression levels of IgE, IL-1β and IL-18 in serum

The increase of serum IgE expression level is one of the key features of AD. After treatment with AESS formula, the expression levels of IL-1β, IgE and IL-18 in serum of mice were determined. The results were shown in Fig. 7B–D. The results showed that compared with the control group, the serum expression levels of IgE, IL-1β and IL-18 in the model group were significantly increased, while compared with model group, the expression levels of IL-1β, IgE and IL-18 in serum of AESS formula group and the DEX group were significantly decreased.

3.3.5. AESS reduced the expression of ASC, Caspase-1 and NLRP3 proteins in skin tissue

In order to investigate whether the mechanism of AESS formula in the treatment of eczema is related to NLRP3 inflammasome, western blot analysis was used to detect the expression levels of NLRP3, ASC and Caspase-1 proteins in skin tissues. Compared with the control group, the expression levels of NLRP3, ASC and Caspase-1 in the model group were significantly increased, while compared with model group, the expression levels of ASC protein and NLRP3 protein in AESS formula group and DEX group were significantly decreased, Caspase-1 protein was significantly decreased in medium and AESS2 group and DEX group, and Caspase-1 protein expression level was slightly decreased in AESS 0.5 group ($p > 0.05$). The results indicated that AESS formula could treat DNCB induced AD like mice by inhibiting the expression of NLRP3 inflammasome (Fig. 8A–D).

4. Discussion

AD is a clinical high incidence of dermatological disease, by a variety of factors act together, stimulate the body to produce an immune response, cytokine expression caused by a delayed abnormal reaction. The disorder of Th1/Th2 balance is the main immunological factor, which is mainly Th1 immune response in the chronic stage and Th2 immune response in the acute stage. IFN-γ secreted by Th1 cells can inhibit Th2 cells, and cytokines secreted by Th2 cells, such as IL-4, IL-5, and IL-13, can induce eosinophilia and increased IgE levels, which restrict each other and maintain the balance. When the body is exposed to allergens, it is easy to react with Th2, stimulate the body's immune cells to

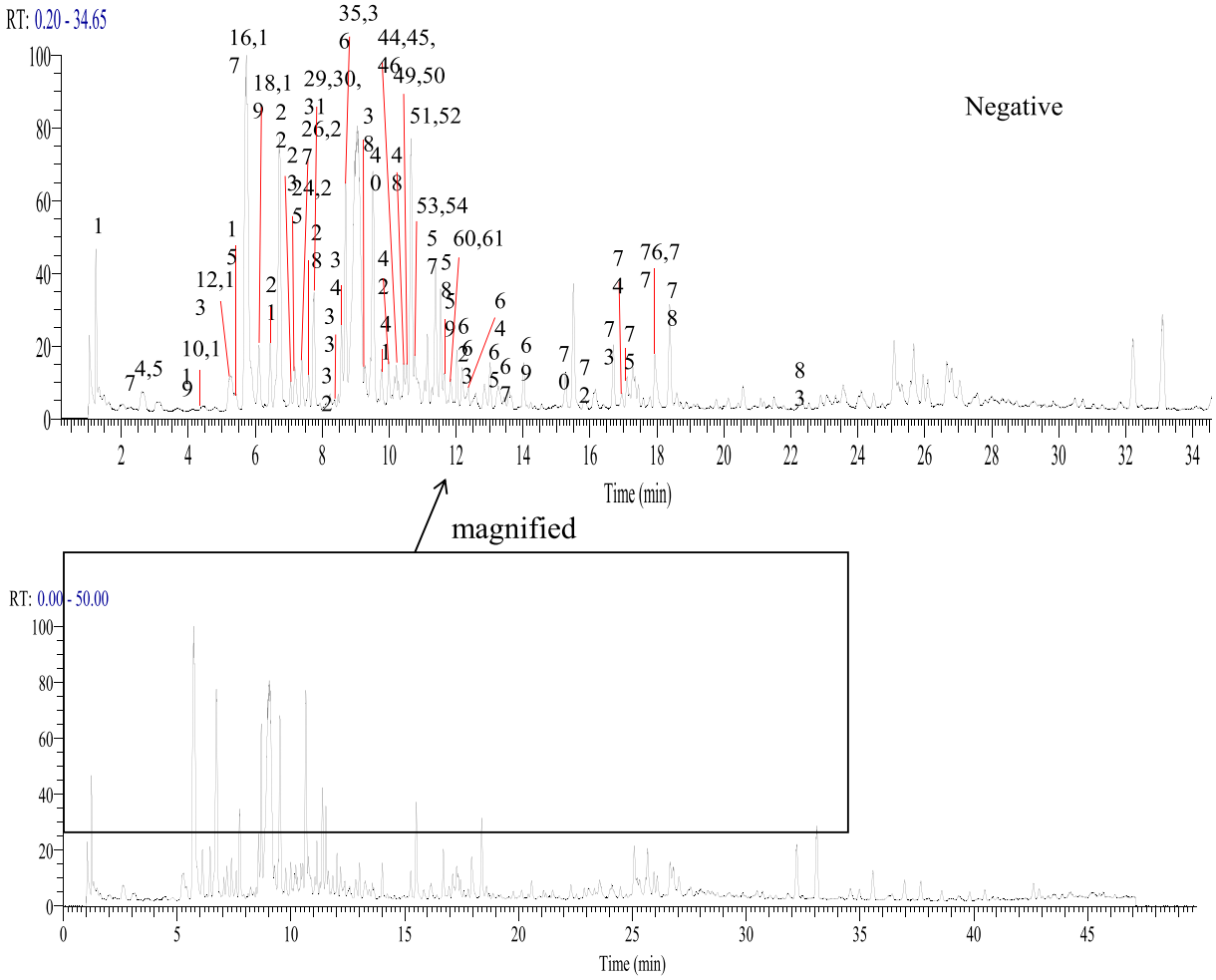

Fig. 1. Total ion chromatography (TIC) of AESS in negative and positive ion modes with amplified part.

secrete IgE and inflammatory cytokines, and trigger allergic reactions by identifying and combining allergens (Zhang et al., 2019a). Multiple factors including race, environment, skin barrier dysfunction, immune regulatory abnormalities, and microbiome have been reported to affect the pathophysiology of AD in a summary of the latest research progress on AD. Progress in the understanding of the immunological mechanisms of AD has found that not only Th1, Th2, but Th17, Th22, and type 2 innate lymphoid cells also contribute to AD (Ahn et al., 2020).

Inherent immunity is an important line of defense for the body against pathogens. Pattern recognition receptors (PRRs) recognize invading microorganisms, dead cell debris or environmental stimuli to activate innate immunity. NLRs are a pattern recognition receptor widely found in the cytosol and are known to be associated with the development of autoimmune diseases such as psoriasis, rheumatoid arthritis and inflammatory bowel disease, and the most studied one is NLRP3 inflammasome (Chen et al., 2021). Recent findings showed that the NLRP3 inflammasome not only is an innate responder to pathogenic and danger signals, but also can affect the adaptive immune response (Chen et al., 2011). IL-18 is an important mediator in the Th1 response, primarily by induction of IFN-γsecretion from T cells and natural killer (NK) cells (Nakanishi et al., 2001). The possible involvement of the NLRP3 inflammasome in Th2 responses was suggested by the fact that IL-33, an IL-1 family cytokine, was shown to be processed by the NLRP3 inflammasome (Ogura et al., 2006). NLRP3 might be involved in Th2 responses, but the role of the NLRP3 inflammasome in type II immune response and AD remains unclear. IL-1β, as a key proinflammatory cytokine in inflammation, was also involved in Th17 cell differentiation (Sutton et al., 2006). IL-1β could synergize with IL-6 to promote Th17 cell development via up-regulation of key IL-17 transcription factors, IRF4 and ROR γt (Chung et al., 2009). DNCB -induced mice model is a classic animal model of AD, and it has been shown to activate the NLRP3 signaling pathway (Liu et al., 2022). When the body is stimulated by DNCB, it sensitizes keratinocytes, and then initiates NLRP3 inflammasome assembly, prompting caspase-1 activation, and then caspase-1 cleaves pro-IL-1β and pro-IL-18 as the active forms IL-1β and IL-18, causing inflammatory response and Th2, Th17-related immune imbalance. Since the NOD-like receptor signaling pathway was deduced to be one of the key pathways by network pharmacological analysis of AESS. Our study shows that AESS formula alleviates symptoms in AD-like mice by regulating the NLRP3 signaling pathway through inhibiting the level expression of IL-1β and IL-18. Reduced IL-1β and IL-18 could restore the Th2 and Th17 immune balance, and thereby alleviate delayed hypersensitivity. Our experiments found that AESS formula regulates the NLRP3 signaling pathway in AD for the first time.

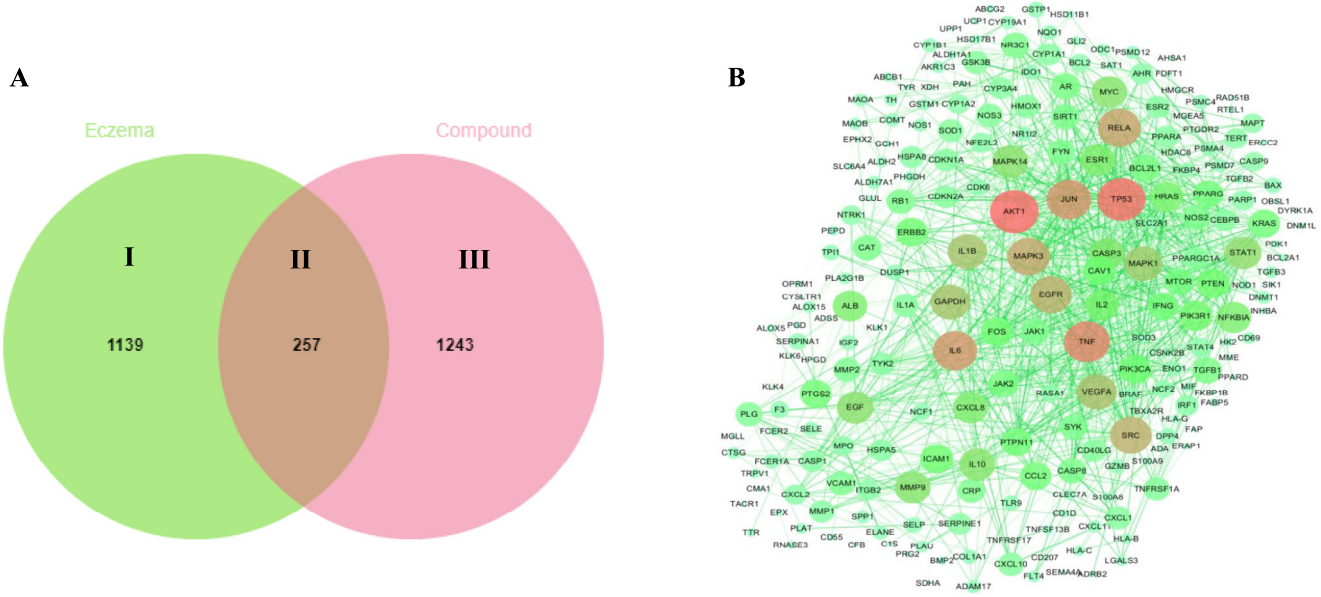

Fig. 2. Venn diagram of the relationship between the target of components of AESS and the target of AD (A) and PPI network of key targets (B). A: I1396 disease targets related to AD, II: 1500 related targets of AESS, III: 257 common targets of components and disease; B: Node color; colored nodes: query proteins and first shell of interactors, white nodes: second shell of interactors, Node content; empty nodes: proteins of unknown 3D structure, filled nodes: some 3D structure is known or predicted, Known Interactions; from curated databases, experimentally determined, Predicted Interactions; gene neighborhood, gene fusions, gene co-occurrence and Others; textmining, coexpression, protein homology.

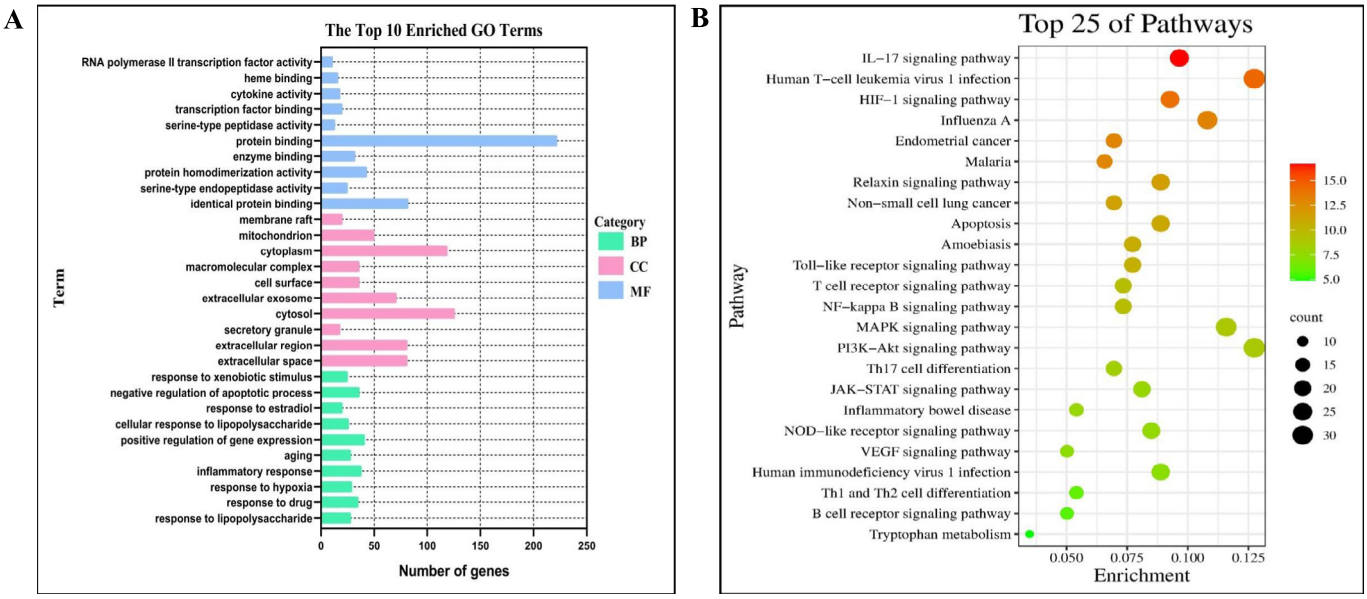

Fig. 3. GO enrichment (A) and KEGG pathway enrichment (B) analysis of core target of AD by AESS (A: The different coloured nodes in the graph indicate the different biological types of GO; B: The nodes in the graph represent the type of KEGG signal pathway. The redder the nodes, the stronger the enrichment significance, and the larger the area, the more the number of enriched genes).

5. Conclusions

In this study, based on systematic chemical profiling and the network pharmacology prediction results, TNF, IL-17, HIF-1, Toll-like receptor, NF-κB and NOD-like receptor signaling pathway were mainly involved, and their related cytokines, such as TNF-α, IL-6, IL-1β, IL-17, etc, influence Th1-Th2, Th17-Treg related immune balance. Most of the main potential bioactive ingredients

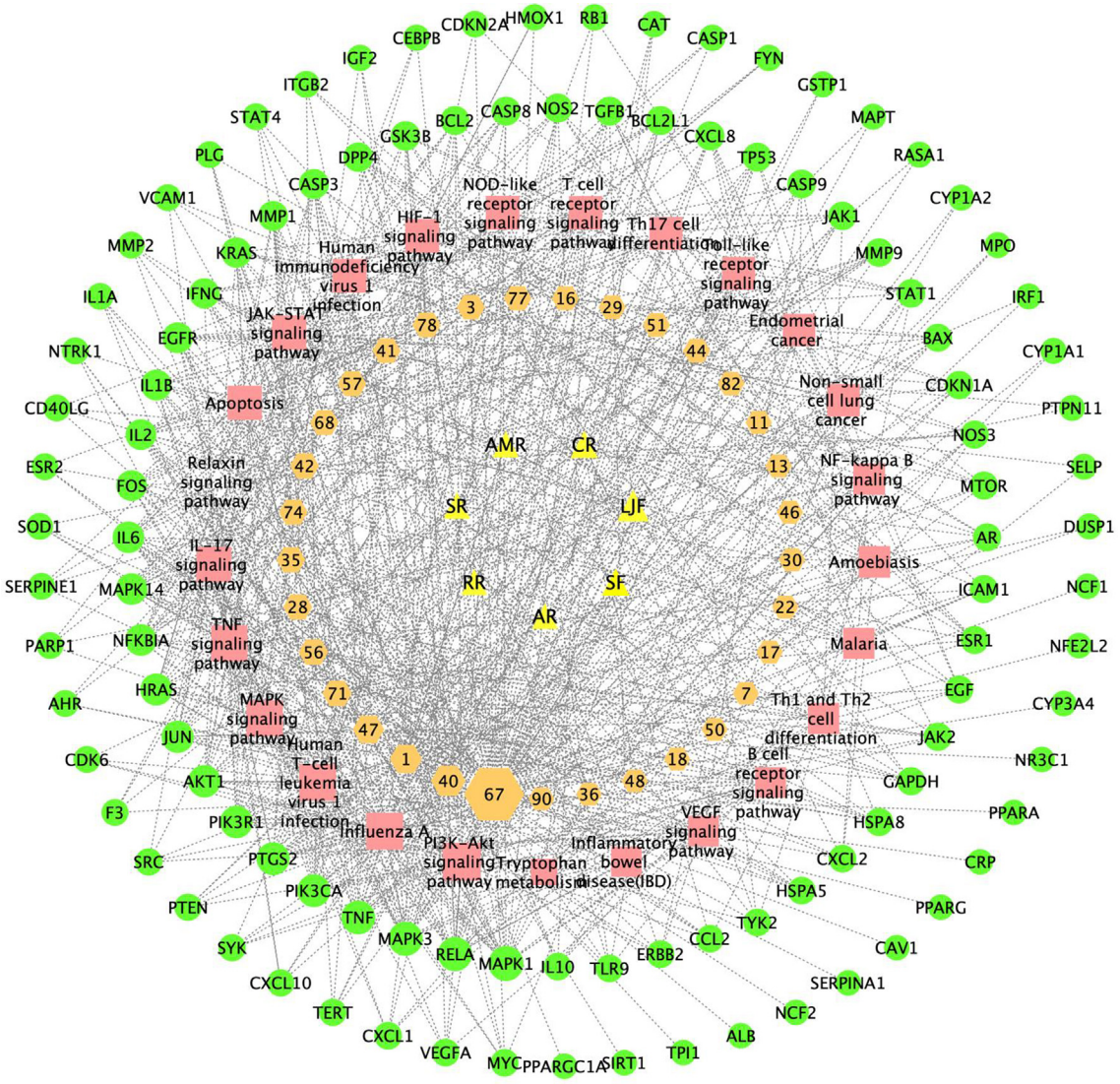

Fig. 4. Network of the herb-component-target-main pathways of AESS (AMR: Atractylodis Macrocephalae Rhizoma; AR: Atractylodis Rhizoma; CR: Curcumae Rhizoma; LJF: Lonicerae Japonicae Flos; SF: Sophorae Flos; RR: Rehmanniae Radix; SR: Saposhnikoviae Radix.

in this formula originated from Lonicerae Japonicae Flos, which further verify its 'Monarch drug' rule. Since NOD-like receptor signaling pathway may be an important mechanism for AESS prescription to treat AD, as testified by animal experiments, the protein expression levels of ASC, Caspase-1, and NLRP3 were significantly increased, demonstrating that NLRP 3 activation promoted eczema symptoms in this mice model. By oral administration of AESS prescription, it improved AD-like symptoms, reduced eosinophil infiltration, reduced scratching behavior, and reduced expression levels of IgE and proinflammatory cytokines in serum, as well as protein expression levels of ASC, Caspase-1, and NLRP3 in skin tissue. These results suggest that AESS prescription can reduce the inflammatory response in DNCB induced AD-like mice by inhibiting the activation of NLRP 3 pathway, which may could provide new therapeutic strategies for the medicine treatment of AD.

Financial support

This work was funded by the National Natural Science Foundation of China Youth Fund (82004364); Second Affiliated Hospital of Guangzhou University of Chinese Medicine (SZ2021ZZ17, SZ2021ZZ39); Guangdong-Hong Kong-Macau Joint Laboratory on Chinese Medicine and Immune Disease Research, Guangzhou University of Chinese Medicine (2020B1212030006); Guangdong Provincial Key Laboratory of Chinese Medicine for Prevention and Treatment of Refractory Chronic Diseases (2018B030322012 and MB2020KF04); Guangzhou Science and Technology Plan Project – Municipal School (College) joint funding project (202201020333). Municipal Schools (Colleges) jointly funded projects (SL2024A03J00887). This work was supported by the Key-Area Research and Development Program of Guangdong Province (No. 2020B1111100010).

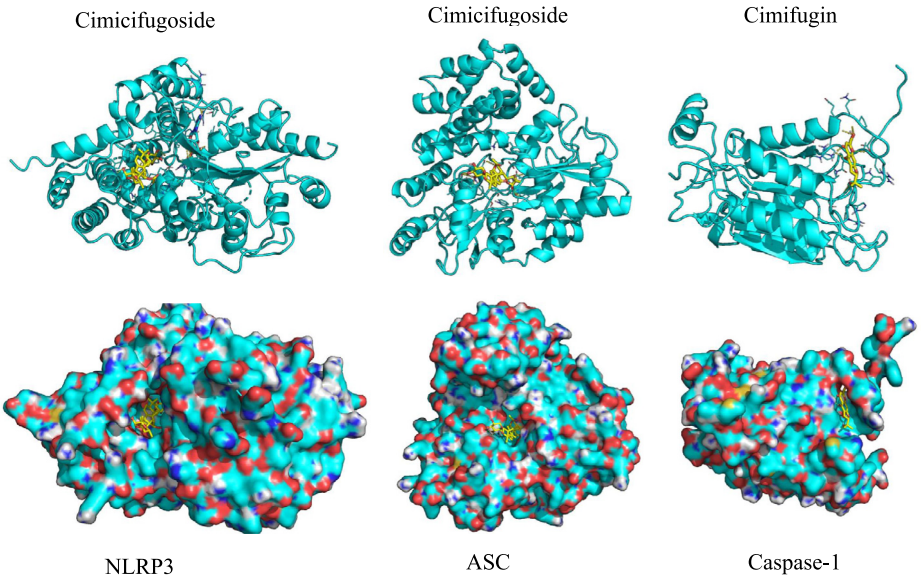

Fig. 5. Molecular docking between the representative small molecule ligands (Cimicifugoside and Cimifugin) and protein (human NLRP3, ASC and Caspase-1), on the top shows the 3D structure of ligands and receptors, at the bottom shows the surface of the receptor and 3D structure of the ligands.

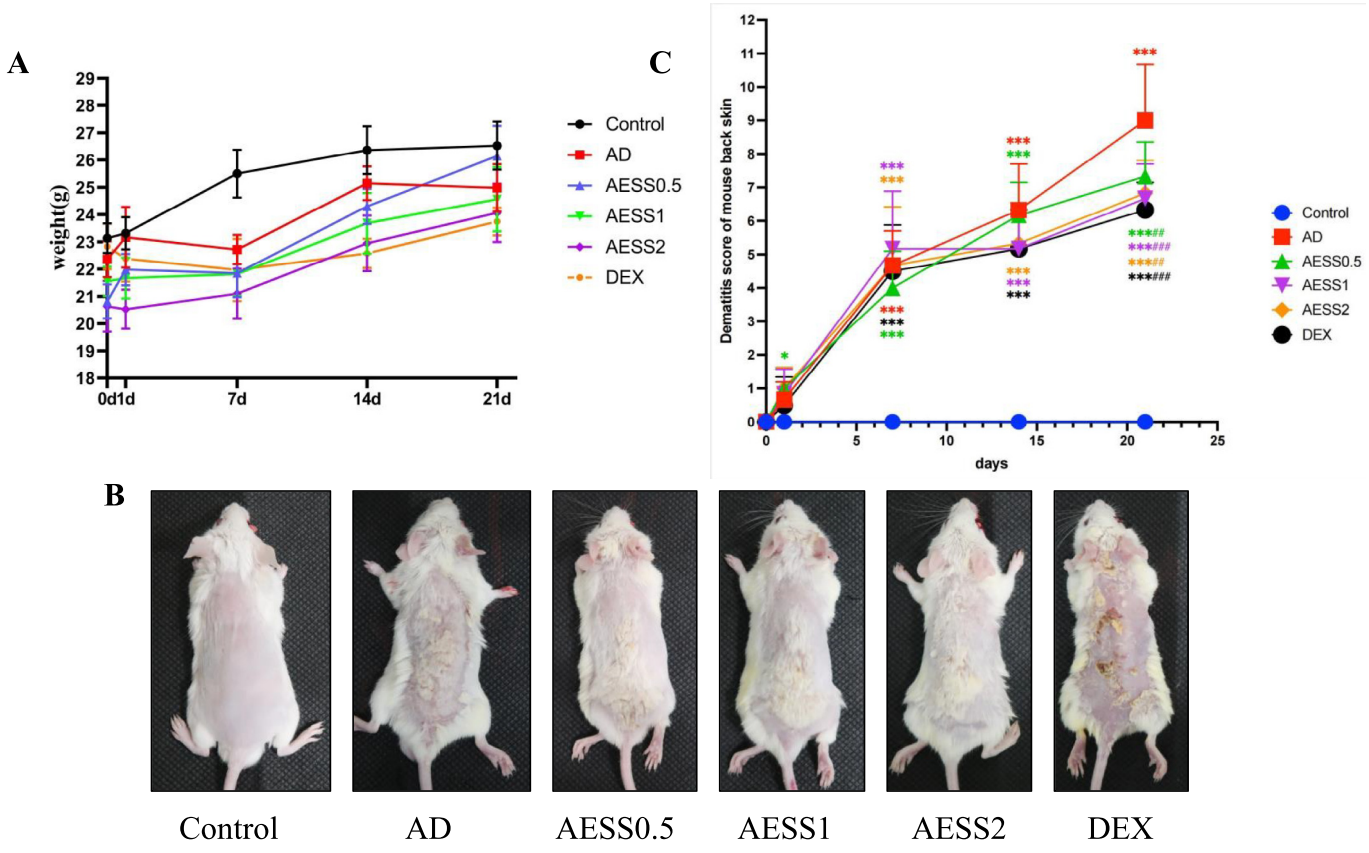

Fig. 6. Treatment with AESS formula inhibits DNCB induced AD-like skin inflammation in BALB/c mice. (A) Changes of body weight in mice. (B) Photograph of the Skin on the Back of Mice. (C) Dermatitis scores in mice. (D) Dermatitis scores in mice. *P < 0.05, **P < 0.01, ***P < 0.001, compared with control group; #P < 0.05, ##P < 0.01, ###P < 0.001, compared with AD group (n = 3–6 per group).

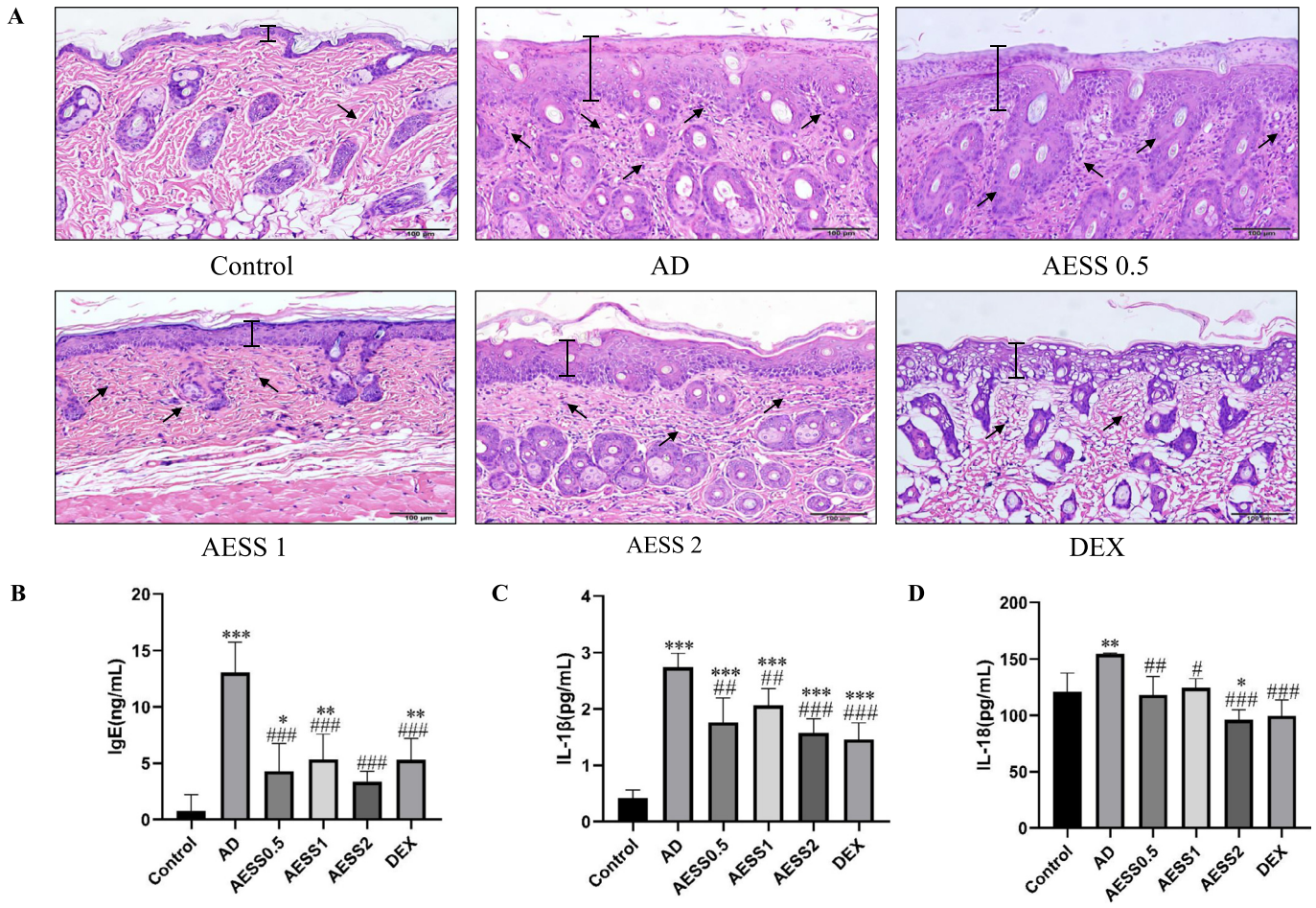

Fig. 7. (A) HE staining for histopathological features (bar length = 100 μm). (B) The serum levels of total IgE in mice. (C) Serum IL-1β expression level. (D) Serum IL-18 expression level. *P < 0.05, **P < 0.01, ***P < 0.001, compared with control group; #P < 0.05, ##P < 0.01, ###P < 0.001, compared with AD group (n = 3–6 per group).

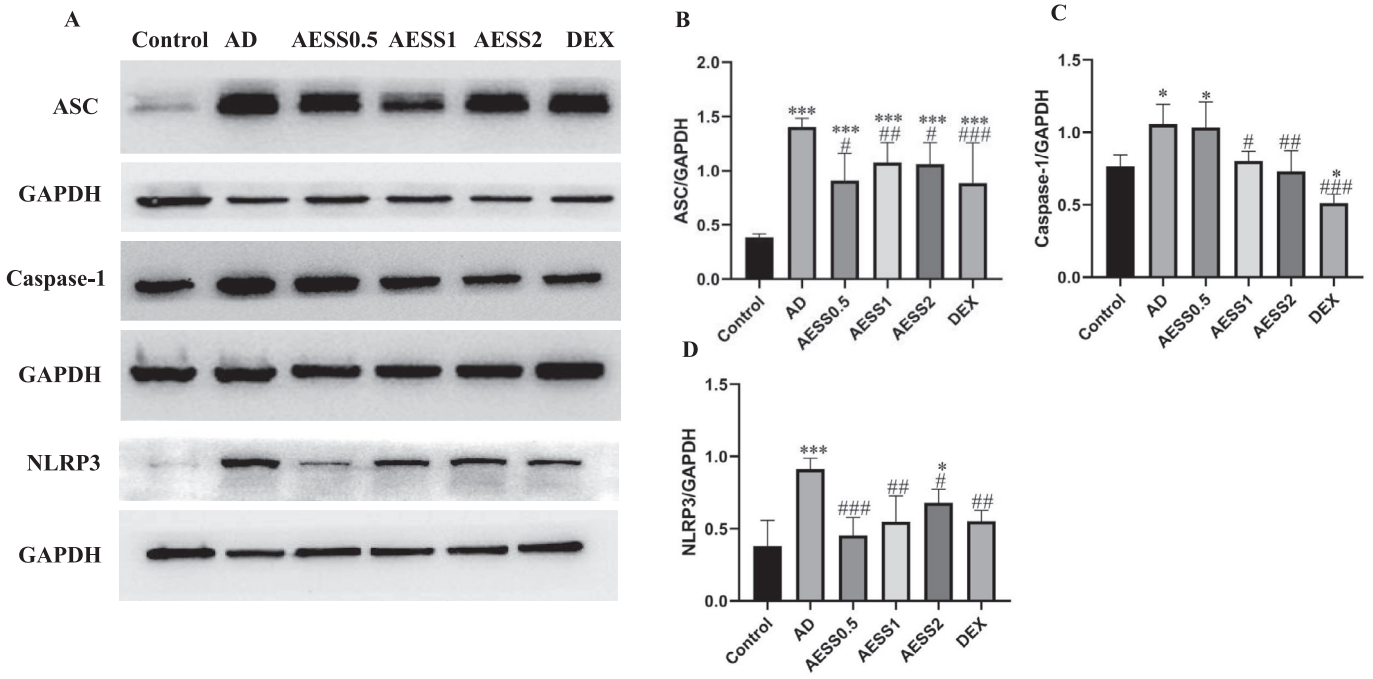

Fig. 8. Western blotting analysis of mouse skin tissue. *P < 0.05, **P < 0.01, ***P < 0.001, compared with control group; #P < 0.05, ##P < 0.01, ###P < 0.001, compared with AD group (n = 3–6 per group).

CRediT authorship contribution statement

Xiong Li: . **Luyao Feng:** . **Tingjing Zhong:** . **Xiumei Mo:** Writing – review & editing. **Dong Wang:** Methodology. **Jiangyong Gu:** . **Dacan Chen:** . **Xing Zeng:** Writing – review & editing. **Fenggen Yan:** .

Declaration of Competing Interest

The authors declare that they have no known competing financial interests or personal relationships that could have appeared to influence the work reported in this paper.

Appendix A. Supplementary material

Supplementary material to this article can be found online at https://doi.org/10.1016/j.jsps.2023.101792.

References

Ahn, K. et al., 2020. Recent advances in atopic dermatitis. Curr. Opin. Immunol. 66, 14–21. https://doi.org/10.1016/j.coi.2020.02.007.

Bylund, S. et al., 2020. Prevalence and Incidence of atopic dermatitis: a systematic review. Acta Derm. Venereol. 100, adv00160. https://doi.org/10.2340/00015555-3510.

Chang, Y.L. et al., 2020. Anti-tumor activity and linear-diarylheptanoids of herbal couple Curcumae Rhizoma-Sparganii Rhizoma and the single herbs. J. Ethnopharmacol. 250, 112465. https://doi.org/10.1016/j.jep.2019.112465.

Chen, M. et al., 2011. Regulation of adaptive immunity by the NLRP3 inflammasome. Int. Immunopharmacol. 11 (5), 549–554. https://doi.org/10.1016/j.intimp.2010.11.025.

Chen, L. et al., 2021. NOD-like receptors in autoimmune diseases. Acta Pharmacol. Sin. 42 (11), 1742–1756. https://doi.org/10.1038/s41401-020-00603-2.

Chung, Y. et al., 2009. Critical regulation of early Th17 cell differentiation by interleukin-1 signaling. Immunity 30, 576–587. https://doi.org/10.1016/j.immuni.2009.02.007.

Dong, Y. et al., 2020. Study on the change of fingerprint and main components of Rhizoma Atractylodis before and after processing. China Pharmacist 12, 2398–2402.

Jia, J. et al., 2022. Therapeutic effect of chinese herbal medicine gu-ben-hua-shi (AESS) formula on atopic dermatitis through regulation of yes-associated protein. Front. Pharmacol. 13, 929580. https://doi.org/10.3389/fphar.2022.929580.

Jiang, Z. et al., 2018. Research progress of external treatment of chronic eczema. Med. Rev. 20, 4103–4107.

Koo, J. et al., 2003. Traditional Chinese medicine in dermatology. Dermatol. Therapy 16, 98–105.

Li, Y. et al., 2019. Rapid identification of chemical constituents of Bushen Huoxue recipe based on UPLC-Q-Exactive quadrupole-electrostatic field orbital trap high resolution mass spectrometry. Chinese J. Pharm. Anal. 01, 111–121. https://doi.org/10.16155/j.0254-1793.2019.01.14.

Li, Z.Y. et al., 2021. Research progress of chemical constituents and pharmacological effects of Rhizoma Curcumae in Guangxi and prediction and analysis of its quality marker (Q-Marker). Chinese Herbal Med. 15, 4687–4699.

Li, H.L. et al., 2022a. Analysis of chemical constituents in different radix curcumae based on UPLC-Q-TOF/MS. Chinese Herbal Med. 11, 2648–2655. https://doi.org/10.13863/j.issn1001-4454.2022.11.021.

Li, S.F. et al., 2022b. Analysis of different processing methods of Flos Lonicerae based on ultra-performance liquid chromatography coupled with high-resolution mass spectrometry. Appl. Chem. 05, 819–827. https://doi.org/10.19894/j.issn.1000-0518.210160.

Liu, W. et al., 2022. Angelica Yinzi alleviates 1-chloro-2,4-dinitrobenzene-induced atopic dermatitis by inhibiting activation of NLRP3 inflammasome and down-regulating the MAPKs/NF-kB signaling pathway. Saudi Pharm. J.: SPJ: Off. Publ. Saudi Pharm. Soc. 30 (10), 1426–1434. https://doi.org/10.1016/j.jsps.2022.07.003.

Lu, X.M. et al., 2023. Based on UHPLC-LTQ-Orbitrap MS, the effects of different processing techniques on the chemical constituents of Rehmannia glutinosa were analyzed. China J. Tradition. Chinese Med. 02, 399–414. https://doi.org/10.19540/j.cnki.cjcmm.20220816.301.

Nakanishi, K. et al., 2001. Interleukin-18 is a unique cytokine that stimulates both Th1 and Th2 responses depending on its cytokine milieu. Cytokine Growth Fact. Rev. 12 (1), 53–72. https://doi.org/10.1016/s1359-6101(00)00015-0.

Ogura, Y. et al., 2006. The inflammasome: first line of the immune response to cell stress. Cell 126 (4), 659–662. https://doi.org/10.1016/j.cell.2006.08.002.

Reuter, J. et al., 2010. Botanicals in dermatology. Am. J. Clin. Dermatol. 11 (4), 247–267.

Schwartz, C. et al., 2018. Spontaneous atopic dermatitis in mice with a defective skin barrier is independent of ILC2 and mediated by IL-1β. Allergy, 1–14. https://doi.org/10.1111/all.13801.

Sutton, C. et al., 2006. A crucial role for interleukin (IL)-1 in the induction of IL-17–producing T cells that mediate autoimmune encephalomyelitis. JEM 203 (7), 1685–1691.

Swanson, K.V. et al., 2019. The NLRP3 inflammasome: molecular activation and regulation to therapeutics. Nature Rev. Immunol. 19 (8), 477–489. https://doi.org/10.1038/s 41577-019-0165-0.

Tanaka, T. et al., 2001. Interleukin-18 is elevated in the sera from patients with atopic dermatitis and from atopic dermatitis model mice, NC/Nga. Int. Arch. Allergy Immunol. 125, 236–240.

Tsang, M.S. et al., 2021. Immunological roles of NLR in allergic diseases and its underlying mechanisms. Int. J. Mol. Sci. 22 (4), 1507. https://doi.org/10.3390/ijms22041507.

Wei, M.J. et al., 2022. Preparation technology of raw rehmannia juice in the classic prescription Lily Rehmannia Decoction based on high resolution mass spectrometry. Chinese J. Exp. Tradition. Med. Formulae 09, 133–140. https://doi.org/10.13422/j.cnki.syfjx.20220616.

Yang, E. et al., 2012. Research progress on chemical constituents and pharmacological effects of Atractylodes macrocephala. J. Guangdong Pharm. Univ. 02, 218–221.

Zhang, Q. et al., 2019a. Research progress on the pathogenesis of atopic dermatitis. World Latest Med. Inf. Abstr. 30, 121–123. https://doi.org/10.19613/j.cnki.1671-3141.2019.30.056.

Zhang, Y. et al., 2019b. Qualitative and quantitative determination of Atractylodes rhizome using ultra-performance liquid chromatography coupled with linear ion trap-Orbitrap mass spectrometry with data-dependent processing. Biomed. Chromatogr.: BMC 33 (3), e4443.

Zhang, Y.H. et al., 2019c. Study on chemical basis and metabonomics of Atractylodes lancea doctoral thesis. Shanghai University of Traditional Chinese Medicine https://kns.cnki.net/kcms2/article/abstract?v=QOR9nnE_NmK2DhimfhVwTpLUMVdbLVslx1rbgkA0I-oQ18SFuzBoWAnS_2hY6lLWTEhqd3IXZ57xO5sua8_PlL8b6nV781YUCR4_MfYQrexDaxHLLabQeHz7SNHYWcKUIT1WUQFIFZ8=&uniplatform=NZKPT&language=CHS.

Zhao, X.F. et al., 2007. HPLC/ESI-MS analysis of Radix Rehmanniae Preparata. Chinese J. Pharm. Anal. 06, 874–876.

Zheng, J. et al., 2021. A novel function of NLRP3 independent of inflammasome as a key transcription factor of IL-33 in epithelial cells of atopic dermatitis. Cell Death Dis. 12 (10), 871. https://doi.org/10.1038/s41419-021-04159-9.

Zhong, Y.M. et al., 2015. Study on rapid identification of chemical constituents of Atractylodes macrocephala based on UPLC/Q-TOFMS technology. Acta Mass Spectromet. 01, 72–77.

Zhou, J. et al., 2020. Analysis of chemical constituents of Atractylodes lancea and Atractylodes macrocephala based on UPLC-QTof-MS/MS. Pharm. Clin. Res. 05, 321–328. https://doi.org/10.13664/j.cnki.pcr.2020.05.001.